Constructing Realistic Canine Bilayer Biatrial Mesh for Atria Fibrillation Simulations

Mirabeau Saha[1,2], Caroline Roney[3], Feng Xiong[1], Hubert Cochet[2], Stephanie Tan[1], Steven Niederer [3], Edward Vigmond[2], and Stanley Nattel[1,2,4]

[1] Department of Medicine and Research Center, Montreal Heart Institute, Montreal, QC, Canada [2] IHU Liryc, Electrophysiology and Heart Modeling Institute, fondation Bordeaux Université, Pessac-Bordeaux, France
[3] Department of Biomedical Engineering, King's College London, London, United Kingdom
[4] Institute of Pharmacology, West German Heart and Vascular Center, University Duisburg-Essen, Essen, Germany

Abstract

Understanding the mechanisms of atrial fibrillation (AF) is essential for improving the diagnostic and therapeutic management of patients. A deeper understanding requires a full appreciation and consideration of the geometry of the atria. Here, we propose the first anatomically accurate high-resolution canine atrial computational bilayer model for AF studies. CT-scan imaging data were segmented and used to distinctly reconstruct 3 main layers representing Bachmann's bundle (BB), the left atrium (LA) and right atrium (RA) with coronary sinus (CS). The LA is dilated to obtain the second layer. The RA endocardial layer consists of the sinus node (SAN), the pectinate muscles (PM) and the crista terminalis (CT). All these parts were combined together and the Ramirez-Nattel-Courtemanche canine cell model was used to simulate electrical activity. Activation time (AT) and action potential duration (APD) were computed. The obtained bilayer mesh has high resolution. The action potential propagation from the SAN was realistic and its path on the real long CS presumes an important role of the CS on the initiation and maintenance of rotors during AF, in agreement with clinical studies. The propagation time from SAN to PVs was ~ 119 *ms and the* APD_{90} *was heterogeneous in the model. This new bilayer model with realistic CS and BB, combined with experimental approaches, will help to better understand AF and its underlying mechanisms, in order to develop better diagnostic and therapeutic options.*

1. Introduction

Atrial fibrillation (AF) is a disorder of the supraventricular rhythm. The atrial remodeling induced by AF itself is an important factor in the natural course of the disease [1]. However, the mechanisms causing this remodeling, whether electrophysiological or structural [2], remain poorly understood. Understanding these mechanisms is however essential to improve the diagnostic and therapeutic management of patients with AF. That understanding requires full and detailed access to the geometry of the atria. Such study in the experimental or clinical configuration is very expensive and complex, and can take a very long-time. Three dimensional mathematical models of the atria are becoming a widely used alternative because different factors can be modified individually or in combination and these experiments are both reproducible and non-invasive. Canine atrial fibrillation exhibits similar properties to human atrial fibrillation and so represents a suitable experimental model. To obtain realistic mathematical models, it is necessary to use data from medical imaging performed on living beings. Recent studies have already shown that CT-Scan is a good modality, very suitable for imaging the canine atria in detail [3, 4]. Various geometrical atrial models have been proposed, indicating the importance of atrial geometry on AF. Human bilayer biatrial model has been recently successfully widely used for AF study [5]. Our laboratory is carrying out numerous AF clinical studies on canine atria. In this study, we have updated the bilayer biatrial model and construct a more detailed and realistic 3D mathematical model of the canine atria geometry for AF studies and the underlying mechanisms. Bilayer 3D models are a compromise between the monolayer and three dimensional models.

2. Methods

A 24.8 Kg dog, 5 years old, was used in this study. The study was approved by the Institutional Ethics Commit-

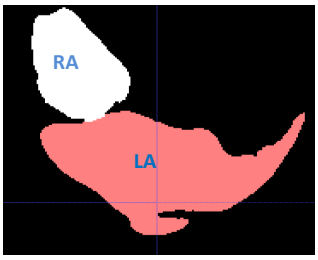

Figure 1: An image slice with the left atrium (LA) segmentation shown in red and right atrium (RA) in white.

tee at the Montreal Heart Institute. The animal was sedated and ventilated during the process with 100% FiO_2. An intravenous access was obtained with an 18-gauge catheter placed in a femoral vein. Beta-blocker (5mg IV q 5 minutes for maximum dose of 15 mg) was given for a heart rate of around 120-140 beat-per-minute. The computed-tomography scan (CT-Scan) was performed using a 128-section dual-source CT system (Somatom Definition Flash; Siemens Medical Solutions, Forchheim, Germany). Images were obtained using an ECG-triggered retrospective axial acquisition from $0\% - 100\%$ of the R-R interval (from the R wave to the next R wave) with a high-pitch and z-axis centered on the heart. CT parameters were as follow: collimation, 2 64.0 0.6 mm; gantry rotation time, 280 ms; temporal resolution, 75 ms; voltage of both tubes, 120kV; current of the tubes, 500mAs for the arterial phase and 450mAs for the late phase. Ventilation was momentarily ceased for the acquisition. Forty-eight milliliters of nonionic, low-ismolar contrast medium (opamidol, Isovue [370 mg iodine per mL]; Bracco) was injected at a rate of 4 mL/s, followed by 10 mL of a 50/50 mix of contrast and normal. Bolus tracking was used with a region of interest placed in the descending aorta and trigger set at 250 HU (Houndsfield Unit). The late phase was acquired immediately after. Reconstruction of both phases were performed at every 5% of the R-R interval field of view limited to the heart with matrix size of $512X512$ pixels, section thickness of 0.75 mm with an increment of 0.3 mm.

2.1. Atria parts extraction, processing and recombination

To remove non atrial structures from DICOM data, volume rendering reconstruction were used as shown on Fig. 1. Then, based on the same protocol we used to obtain human patient-specific bilayer biatrial model [6], the right atrium (RA) epicardial layer, the left atrium (LA) and the Bachmann's bundle (BB) endocardial surfaces were obtained from manual segmentation using ITK-Snap tool. The RA part includes a long coronary sinus (CS). Each part is then meshed, smoothed and trimmed. The Fossa Ovalis (FO) position was identified on each atrium. RA extra parts such the sinoatrial node (SAN), the pectinate muscles (PM) and the crista terminalis (CT) are computed from connection points and included in the RA as endocardial layer. Fedorov et al. [7] found experimentally a block zone near the SAN. That block zone was implemented in this bilayer model. The LA endocardial layer is dilated to construct the LA epicardial layer. The fiber directions were assigned to each part of the model using the same approach as in the previous study [8]. Figure 2 shows fiber directions on the model parts. BB and FO connect RA to LA manually using extra triangular elements. The RA is also manually connected to the LA through CS using triangular elements. Both LA layers are joined each other by discrete linear electrical connections.

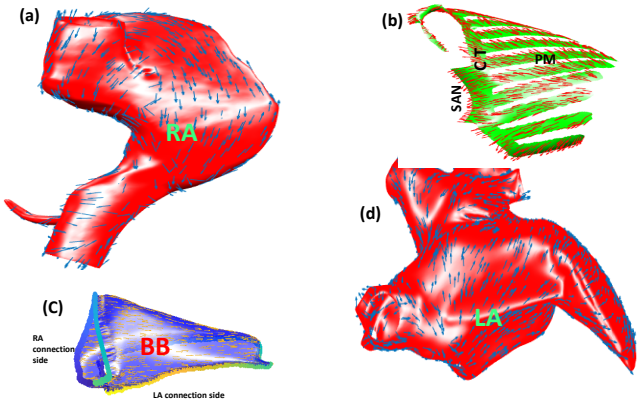

Figure 2: Atria parts with fiber directions. For viewing purposes, 1/100 fibers represented on RA **(a)**, 1/5 on SAN, CT and PMs **(b)**, 1/20 on BB **(c)** and 1/100 on bilayer LA

2.2. Electro-physiological simulation

To test the model, the Ramirez-Nattel-Courtemanche canine cell model [9] was used for simulations. The monodomain equation was used to describe the electrical propagation propagation and solved using the finite element method. Ionic properties and conductivities were adjusted to achieve realistic propagation speeds. A passive ionic model was used in the inferior veina cava (IVC) and the block regions with a resting level -83 mV. Sinus activation was simulated by stimulating the SAN nodes with 27 mV stimuli at 1.67Hz and the activation time (AT) to the pulmonary veins (PVs) and LA appendage (LAA) was measured. The action potential duration at 90% repolarization (APD_{90}) was computed on each node of the mesh.

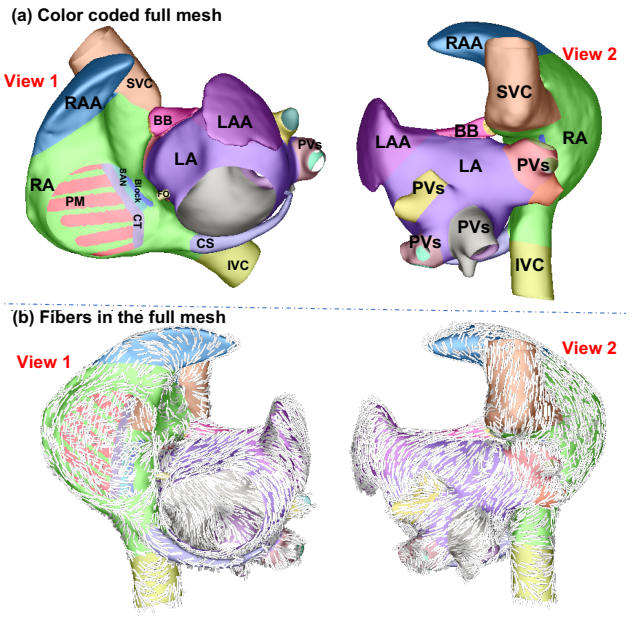

Figure 3: Canine specific bilayer atria model with regions colors coded. **b** Fiber directions in the mesh.

3. Results and discussion

Figure 3(**a**), with region coded, represents the resulting canine-specific bilayer biatrial mesh. Figure 3(**b**) shows the full mesh including the fiber directions (where 1/100 fibers are represented). It contains 1179133 nodes, 2346395 triangular elements in total, 350909 line elements to couple LA layers together and 353445 line elements in total in the model. The average edge length is $276.25 \pm 57.55 \mu m$. The model has the four usual PVs and an extra one in the middle left. With five pulmonary veins, this mesh is from a dog with particular atria geometry. This is the first realistic canine bilayer biatria mesh, the first bilayer mesh with a long realistic CS. Previous studies have suggested that the CS may play a role in perpetuating AF [10] and it can be target for permanent atrial fibrillation ablation therapy [11]. But the exact roles of CS in AF initiation and perpetuation are not completely elucidated. This new model will help to better investigate the role of CS in the AF.

The propagation of the electrical activity from the SAN went around the block zone, thus undergoing a delay. The propagation continued through BB and FO to reach LA. The total propagation time over the mesh, to reach the last node on PVs, was $\sim$ 118.54 ms as shown on Fig. 4. As illustrated on Fig. 5, APD90 was $\sim$ 108.21 ms on the PVs, $\sim$ 127.90 ms on the LAA, $\sim$ 133.94 ms on the LA, $\sim$ 139.38 ms on RAA, $\sim$ 145.67 ms on the RA, $\sim$ 196.02 ms on BB and CT, $\sim$ 158.49 ms on PM and

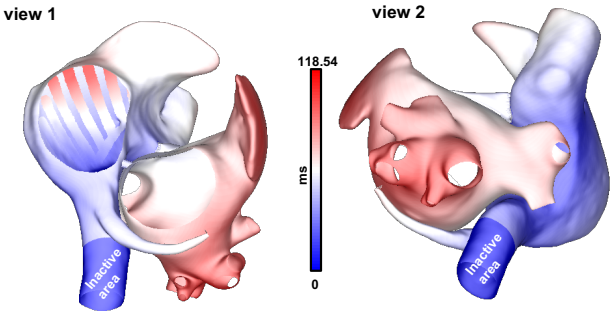

Figure 4: Activation time (AT) map showing propagation from SAN to PVs and LAA tip.

$\sim$ 235.81 ms on SAN. These results are in agreement with activation time mesured experimentally [9, 12]. It is known that the intrinsic APD heterogeneity between atria regions as obtained in this study can translate into slowing of the AP conduction velocity in regions with relatively long refractoriness [3, 9]. Such electrical heterogeneities play an important role on the AF dynamics.

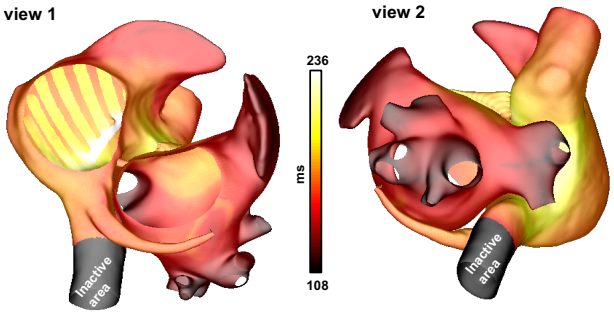

Figure 5: Action potential duration (APD_{90}) map.

4. Conclusion

In this work, we have built the first canine specific realistic bilayer biatrial model. Since this model can significantly reduce computation time while retaining valuable features affecting propagation, it is a good trade-off between the limited monolayer model and the volumetric model which requires an important computational load. It will help for studying AF dynamics as well as testing various ablation strategies.

Acknowledgments

For this study, computer time was partially provided by the computing facilities Cedar on Compute Canada.

References

[1] Nattel S, Harada M. Atrial remodeling and atrial fibrillation: recent advances and translational perspectives. Journal of the American College of Cardiology 2014; 63(22):2335–2345.

[2] Schotten U, Verheule S, Kirchhof P, Goette A. Pathophysiological mechanisms of atrial fibrillation: a translational appraisal. Physiological reviews 2011;91(1):265–325.

[3] Aslanidi OV, Nikolaidou T, Zhao J, Smaill BH, Gilbert SH, Holden AV, Lowe T, Withers PJ, Stephenson RS, Jarvis JC, et al. Application of micro-computed tomography with iodine staining to cardiac imaging, segmentation, and computational model development. IEEE transactions on medical imaging 2012;32(1):8–17.

[4] Genain MA, Morlet A, Herrtage M, Muresian H, Anselme F, Latremouille C, Laborde F, Behr L, Borenstein N. Comparative anatomy and angiography of the cardiac coronary venous system in four species: human, ovine, porcine, and canine. Journal of Veterinary Cardiology 2018;20(1):33–44.

[5] Roney CH, Ng FS, Debney MT, Eichhorn C, Nachiappan A, Chowdhury RA, Qureshi NA, Cantwell CD, Tweedy JH, Niederer SA, et al. Determinants of new wavefront locations in cholinergic atrial fibrillation. EP Europace 2018; 20(suppl_3):iii3–iii15.

[6] Labarthe S, Bayer J, Coudière Y, Henry J, Cochet H, Jaïs P, Vigmond E. A bilayer model of human atria: mathematical background, construction, and assessment. Europace 2014; 16(suppl_4):iv21–iv29.

[7] Fedorov VV, Schuessler RB, Hemphill M, Ambrosi CM, Chang R, Voloshina AS, Brown K, Hucker WJ, Efimov IR. Structural and functional evidence for discrete exit pathways that connect the canine sinoatrial node and atria. Circulation research 2009;104(7):915–923.

[8] Roney CH, Williams SE, Cochet H, Mukherjee RK, O'Neill L, Sim I, Whitaker J, Razeghi O, Klein GJ, Vigmond EJ, et al. Patient-specific simulations predict efficacy of ablation of interatrial connections for treatment of persistent atrial fibrillation. EP Europace 2018;20:iii55–iii68.

[9] Ramirez RJ, Nattel S, Courtemanche M. Mathematical analysis of canine atrial action potentials: rate, regional factors, and electrical remodeling. American Journal of Physiology Heart and Circulatory Physiology 2000; 279(4):H1767–H1785.

[10] Oral H, Ozaydin M, Chugh A, Scharf C, Tada H, Hall B, Cheung P, PELOSI Jr F, Knight BP, Morady F. Role of the coronary sinus in maintenance of atrial fibrillation. Journal of cardiovascular electrophysiology 2003;14(12):1329–1336.

[11] Ahmed N, Rungatscher A, Linardi D, Molon G, Luciani GB, Faggian G. Pp-158 coronary sinus can be target for permanent atrial fibrillation ablation therapy? American Journal of Cardiology 2016;117:S98.

[12] Ehrlich JR, Cha TJ, Zhang L, Chartier D, Melnyk P, Hohnloser SH, Nattel S. Cellular electrophysiology of canine pulmonary vein cardiomyocytes: action potential and ionic current properties. The Journal of physiology 2003; 551(3):801–813.

Address for correspondence:

Mirabeau Saha
Montreal Heart Institute, 5000 Rue Bélanger, S4501, Montreal, Quebec, H1T 1C8, Canada
mirabeau.saha@mail.mcgill.ca